

# The Critical End Point of Quantum Chromodynamics Detected by Chirally Imbalanced Quark Matter

Marco Ruggieri

*Yukawa Institute for Theoretical Physics, Kyoto University,  
Kitashirakawa Oiwake-cho, Sakyo-ku, Kyoto 606-8502, Japan.*

We suggest the idea, supported by concrete calculations within chiral models, that the critical endpoint of the phase diagram of Quantum Chromodynamics with three colors can be detected, by means of Lattice simulations of grand-canonical ensembles with a chiral chemical potential,  $\mu_5$ , conjugated to chiral charge density. In fact, we show that a continuation of the critical endpoint of the phase diagram of Quantum Chromodynamics at finite chemical potential,  $\mu$ , to a critical end point in the temperature-chiral chemical potential plane, is possible. This study paves the way of the mapping of the phases of Quantum Chromodynamics at finite  $\mu$ , by means of the phases of a fictitious theory in which  $\mu$  is replaced by  $\mu_5$ .

PACS numbers: 12.38.Aw, 12.38.Mh, 12.38.Lg

Keywords: Effective Models of QCD, Critical Endpoint of the QCD Phase Diagram.

## I. INTRODUCTION

The critical endpoint, CP, of Quantum Chromodynamics (QCD) [1] is one of the most important aspects of the phase diagram of strongly interacting matter. It is thus not surprising that an intense experimental activity is nowadays dedicated to the detection of such a point, which involves the large facilities at RHIC and LHC; moreover, further experiments are expected after the development of FAIR at GSI. Several theoretical signatures of CP have been suggested [2, 3]. Despite the importance of CP, a firm theoretical evidence of its existence is still missing. In fact, the sign problem makes the Lattice Monte Carlo simulations difficult, if not impossible, in the large baryon-chemical potential ( $\mu$ ) region for  $N_c = 3$  [4], see [5] for a recent review. Therefore, it has not yet been possible to prove unambiguously the existence and the location of CP starting from first principles simulations of grand-canonical ensembles. The strong coupling expansion of Lattice QCD [6, 7] seems promising. Even more, the predictions of effective models are spread in the  $T - \mu$  plane, see for example [8, 9].

An interesting overcoming of the sign problem for the quest of CP is offered by analytic continuation of data obtained at imaginary chemical potential,  $\mu_I$  [10–12]. Recent promising analysis shows that it might be possible to continue the critical line from the region of imaginary  $\mu$  to that of real  $\mu$  [13], pinning down the critical point. Another fruitful approach is given by simulations at finite isospin chemical potential,  $\delta\mu$ , see for example [14–16]. Even in this case, a critical endpoint there appears before the transition to the pion condensed phase. The latter point has been overlooked and it has not yet been detected by mean field model calculations; hence it certainly deserves further study. It is also worth to cite the possibility to perform simulations in canonical, rather than grand-canonical, ensembles. Preliminary results in this direction have been presented recently in [17]. On the purely theoretical side, it has been suggested very

recently [18] that the use of orbifold equivalence in the large  $N_c$  approximation of QCD can lead to relations between the coordinates of CP at finite chemical potential, with those at finite isospin chemical potential.

In this Article, we suggest a new, theoretical way to detect the CP, by means of Lattice simulations with  $N_c = 3$ , which can be considered as an alternative to the  $\mu_I$  technique. In order to accomplish this important program, we suggest to simulate QCD with a chiral chemical potential,  $\mu_5$ , conjugated to the chiral charge density,  $n_5 = n_R - n_L$ , see [19–22] for previous studies. Our idea, supported by concrete calculations within microscopic effective models, is that CP can be *continued* to a critical endpoint at  $\mu_5 \neq 0$  and  $\mu = 0$ , that we denote by  $CP_5$ , the latter being accessible to  $N_c = 3$  Lattice QCD simulations of grand-canonical ensembles [19]. Therefore, the detection of the former endpoint via Lattice simulations, can be considered as a signal of the existence of the latter. To facilitate exposition, we introduce the symbol  $\mathcal{W}_5$  to denote the world with  $\mu = 0$ ,  $\mu_5 \neq 0$ . On the other hand, we will use the symbol  $\mathcal{W}$  to denote the world with  $\mu_5 = 0$ , and which corresponds to the physical universe.

The model calculations, in particular the ones based on the Nambu-Jona-Lasinio model with the Polyakov loop [23] (PNJL model in the following) with tree level coupling among chiral condensate and Polyakov loop [24], give numerical relations among the coordinates of  $CP_5$  and those of CP. In particular, the critical temperature turns out to be almost unaffected by the process of continuation; the critical value of the chemical potential,  $\mu_c$ , on the other hand turns out to be almost half of the critical chiral chemical potential,  $\mu_{5c}$ .

Before discussing our results, it is important to spend some word more about the chiral chemical potential. In particular, we are aware that  $\mathcal{W}_5$  should be considered as a fictional universe. As a matter of fact,  $\mu_5$  cannot be considered as a true chemical potential because, in the confinement phase, the chiral condensate  $\langle \bar{q}q \rangle$  mixes left- and right-handed components of the quark field, leading to non-conservation of  $n_5$ . This statement is true also

in the Quark-Gluon-Plasma phase, where the chiral condensate is much smaller than its value in the confinement phase; in this case, the non-conservation of  $n_5$  is much softer, and mainly due to the bare quark mass,  $m \ll T$  with  $T$  corresponding to the temperature of the heat bath in which the fields live. Therefore, the point of view that we adopt in this Article is to consider  $\mu_5$  as a mere mathematical artifice. However,  $\mathcal{W}_5$  with  $N_c = 3$  can be simulated on the Lattice. Therefore, for the continuity property cited above, it is worth to study it by grand-canonical ensemble simulations: it might furnish an evidence of the existence of the critical endpoint in the real world. Furthermore, once  $\text{CP}_5$  is detected, it might be possible to make use of Lattice simulations to detect inhomogeneous phases [25, 26] which could develop around  $\text{CP}_5$ , as a continuation of those which develop at CP. The results would then be of vital importance to understand, for example, the inner structure of compact stellar objects. For the aforementioned reasons, this study is very far from being of purely academic or theoretical interest.

## II. CHIRAL MODELS

Because of its non-perturbative nature, we cannot make first principles calculations within QCD in the regimes to which we are interested in, namely moderate  $T$ ,  $\mu$  and  $\mu_5$ . Hence we need to rely on some effective model, which is built in order to respect (at least some of) the symmetries of the QCD action. To this end, we make use of the celebrated Quark-Meson model [27], and of the Nambu-Jona-Lasinio model [28] (see [29] for reviews) improved with the Polyakov loop [23], dubbed PNJL model, which have been used many times in recent years to describe successfully the thermodynamics of QCD with two and two-plus-one flavors, see [24, 30–37] and references therein. They are interesting because they allow for a self-consistent description of spontaneous chiral symmetry breaking; even more, in the case the model is improved with the Polyakov loop, it allows for a simultaneous computation of quantities sensible to confinement and chiral symmetry breaking.

In this Section we describe both of the models. We firstly discuss the Quark-Meson model that we use in our computation, which is simpler to implement since take its simplest version, without the complications due to the finite value of the quark masses and to the Polyakov loop. This is an useful preparation to the more important case of the PNJL model, which is more trustable quantitatively since it is tuned to reproduce Lattice data at zero and imaginary chemical potential.

### A. Quark-Meson Model

The Quark-Meson (QM) model consists of the  $O(4)$  linear sigma model coupled to dynamical quarks via a Yukawa-type interaction. The lagrangian density is given

by

$$\mathcal{L} = \bar{q} [i\partial_\mu \gamma^\mu - g(\sigma + i\gamma_5 \boldsymbol{\tau} \cdot \boldsymbol{\pi}) + \mu_5 \gamma^0 \gamma^5 + \mu \gamma^0] q + \frac{1}{2} (\partial_\mu \sigma)^2 + \frac{1}{2} (\partial_\mu \boldsymbol{\pi})^2 - U(\sigma, \boldsymbol{\pi}) . \quad (1)$$

In the above equation,  $q$  corresponds to a quark field in the fundamental representation of color group  $SU(3)$  and flavor group  $SU(2)$ ; besides,  $\sigma$  and  $\boldsymbol{\pi}$  correspond to the scalar singlet and the pseudo-scalar iso-triplet fields, respectively. We have introduced chemical potential for the quark number density,  $\mu$ , and a pseudo-chemical potential conjugated to chirality imbalance,  $\mu_5$ .

We explain in some detail the physical meaning of the latter. The quantity conjugated to  $\mu_5$ , namely the chiral charge density, is given by  $n_5 = n_R - n_L$ , and represents the difference in densities of the right- and left-handed quarks. At finite  $\mu_5$ , a chirality imbalance is created, namely  $n_5 \neq 0$ . For example, in the massless limit and at zero baryon chemical potential one has [19]

$$n_5 = \frac{\mu_5^3}{3\pi^2} + \frac{\mu_5 T^2}{3} . \quad (2)$$

If quark mass (bare or constituent) is taken into account, the relation  $n_5(\mu_5)$  cannot be found analytically in the general case, and a numerical investigation is needed, see for example [20]. The imbalance of chiral density can be created by instanton/sphaleron transition in QCD, see [19] and references therein. As a matter of fact, non perturbative background gluon configurations with nonzero winding number,  $Q_W$ , change the chirality of quarks according to the Ward identity:

$$\frac{dn_5}{dt} = -\frac{g^2 N_f}{16\pi^2} \int d^3x F_{\mu\nu}^a \tilde{F}_a^{\mu\nu} = -\frac{Q_W}{2N_f} . \quad (3)$$

As a consequence, the addition of  $\mu_5$  to the lagrangian density of the chiral models mimics the instanton/sphaleron induced chirality transitions.

The potential  $U$  describes tree-level interactions among the meson fields. In this Article, we restrict ourselves to the QM model in the chiral limit for simplicity, and take

$$U(\sigma, \boldsymbol{\pi}) = \frac{\lambda}{4} (\sigma^2 + \boldsymbol{\pi}^2 - v^2)^2 , \quad (4)$$

which is invariant under the chiral group.

We work in the one-loop approximation, which amounts to consider mesons as classical fields, and integrate only over fermions in the generating functional of the theory to obtain the Quantum Effective Potential (QEP). In the integration process, the meson fields are fixed to their classical expectation values,  $\langle \boldsymbol{\pi} \rangle = 0$  and  $\langle \sigma \rangle \neq 0$ . The physical value of  $\langle \sigma \rangle$  will be then determined by minimization of the QEP. The field  $\sigma$  has the quantum numbers of the QCD chiral condensate,  $\langle \bar{q}q \rangle$ . Hence its non-vanishing expectation value breaks chiral symmetry spontaneously, mimicking the chiral symmetry breaking of the QCD vacuum.

The one-loop QEP in presence of  $\mu_5$  has been discussed several times [19–21]. The addition of the  $\mu$ -dependence is a textbook matter. The final result is

$$V = U - N_c N_f \sum_{s=\pm 1} \int \frac{d^3 \mathbf{p}}{(2\pi)^3} \omega_s - \frac{N_c N_f}{\beta} \sum_{s=\pm 1} \int \frac{d^3 \mathbf{p}}{(2\pi)^3} \log \left( 1 + e^{-\beta(\omega_s - \mu)} \right) - \frac{N_c N_f}{\beta} \sum_{s=\pm 1} \int \frac{d^3 \mathbf{p}}{(2\pi)^3} \log \left( 1 + e^{-\beta(\omega_s + \mu)} \right), \quad (5)$$

where

$$\omega_s = \sqrt{(|\mathbf{p}|s - \mu_5)^2 + m_q^2}, \quad (6)$$

corresponds to the pole of the quark propagator, and  $m_q = g\sigma$  is the constituent quark mass; finally, the index  $s$  denotes the helicity projection.

In right hand side of the first line of Equation (5) the momentum integral corresponds to the vacuum quark fluctuations contribution to the QEP. It is divergent, and it gives a contribution at  $T = 0$  and  $\mu_5 \neq 0$ . For our purposes, it is enough to treat the model as an effective description of the infrared regime of QCD. Therefore we treat the divergence phenomenologically, introducing a momentum cutoff,  $M$ , in the vacuum term. This is equivalent to introduce a momentum-dependent quark mass, which is nonzero and constant for momenta lower than the cutoff, and zero for larger values of momenta, thus realizing a rough approximation of the effective (momentum-dependent and ultraviolet suppressed) quark mass of full QCD [38].

The parameters of the model are tuned as in [9]. They are chosen in order to satisfy the requirements that  $\sigma = f_\pi$  in the vacuum,

$$\left. \frac{\partial V}{\partial \sigma} \right|_{\sigma=f_\pi} = 0, \quad (7)$$

and  $m_\sigma = 700$  MeV, where

$$\left. \frac{\partial^2 V}{\partial \sigma^2} \right|_{\sigma=f_\pi} = m_\sigma^2, \quad (8)$$

Moreover, the constituent quark mass in the vacuum is fixed to the value  $m_q = 335$  MeV, which allows to fix the numerical value of  $g = m_q/f_\pi$  with  $f_\pi = 92.4$  MeV. Finally, the ultraviolet cutoff is taken  $M = 600$  MeV. This procedure fixes  $\lambda = 2.73$  and  $v^2 = -(617.7 \text{ MeV})^2$ .

## B. PNJL model

In the PNJL model, quark propagation in the medium is described by the following lagrangian density:

$$\mathcal{L} = \bar{q} (i\gamma^\mu D_\mu - m) q + \mathcal{L}_I; \quad (9)$$

here  $q$  is the quark Dirac spinor in the fundamental representation of the flavor  $SU(2)$  and the color group;  $\boldsymbol{\tau}$  correspond to the Pauli matrices in flavor space. A sum over color and flavor is understood. The covariant derivative embeds the QCD coupling with the background gluon field which is related to the Polyakov loop, see below. Furthermore, we have defined

$$\mathcal{L}_I = G \left[ (\bar{q}q)^2 + (i\bar{q}\gamma_5 \boldsymbol{\tau}q)^2 \right]. \quad (10)$$

One advantage to use the PNJL model is that it has access to the expectation value of the Polyakov loop, that we denote by  $L$ , which is sensible to confinement or deconfinement properties of a given phase. In order to compute  $L$  we introduce a static, homogeneous and Euclidean background temporal gluon field,  $A_0 = iA_4 = i\lambda_a A_4^a$ , coupled minimally to the quarks via the QCD covariant derivative [23]. Then

$$L = \frac{1}{3} \text{Tr}_c \exp(i\beta\lambda_a A_4^a), \quad (11)$$

where  $\beta = 1/T$ . In the Polyakov gauge, which is convenient for this study,  $A_0 = i\lambda_3\phi + i\lambda_8\phi^8$ ; moreover, for simplicity we take  $L = L^\dagger$  from the beginning as in [30], which implies  $A_4^8 = 0$ . We have then

$$L = \frac{1 + 2 \cos(\beta\phi)}{3}. \quad (12)$$

For our purpose, that is mainly the location of the critical endpoint, we expect that the approximation  $L = L^\dagger$  is sufficient; as a matter of fact, we have verified that in this case we reproduce, at finite  $\mu$ , the location of the critical endpoint obtained in [24], where the same parametrization of the model is used, and where  $L \neq L^\dagger$  from the beginning.

In our computation we follow the idea implemented in [24], which brings to a Polyakov-loop-dependent coupling constant:

$$G = g \left[ 1 - \alpha_1 L L^\dagger - \alpha_2 (L^3 + (L^\dagger)^3) \right], \quad (13)$$

The ansatz in the above equation was inspired by [39, 40] in which it was shown explicitly that the NJL vertex can be derived in the infrared limit of QCD, it has a non-local structure, and it acquires a non-trivial dependence on the phase of the Polyakov loop. We refer to [24] for a more detailed discussion. This idea has been analyzed recently in [41], where the effect of the confinement order parameter on the four-fermion interactions and their renormalization-group fixed-point structure has been investigated. The numerical values of  $\alpha_1$  and  $\alpha_2$  have been fixed in [24] by a best fit of the available Lattice data at zero and imaginary chemical potential of Ref. [42, 43]. In particular, the fitted data are the critical temperature at zero chemical potential, and the dependence of the Roberge-Weiss endpoint on the bare quark mass. The best fit procedure leads to  $\alpha_1 = \alpha_2 \equiv \alpha = 0.2 \pm 0.05$ ,

within the hard cutoff regularization scheme, which is the same scheme that we adopt in this Article.

In the one-loop approximation, the effective potential of this model is given by

$$V = \mathcal{U}(L, L^\dagger, T) + \frac{\sigma^2}{G} - N_c N_f \sum_{s=\pm 1} \int \frac{d^3 \mathbf{p}}{(2\pi)^3} \omega_s - \frac{N_c N_f}{\beta} \sum_{s=\pm 1} \int \frac{d^3 \mathbf{p}}{(2\pi)^3} \log(F_+ F_-) \quad (14)$$

where

$$F_- = 1 + 3L e^{-\beta(\omega_s - \mu)} + 3L^\dagger e^{-2\beta(\omega_s - \mu)} + e^{-3\beta(\omega_s - \mu)}, \quad (15)$$

$$F_+ = 1 + 3L^\dagger e^{-\beta(\omega_s + \mu)} + 3L e^{-2\beta(\omega_s + \mu)} + e^{-3\beta(\omega_s + \mu)}, \quad (16)$$

denote the statistical confining thermal contributions to the effective potential;  $\omega_s$  is still given by Equation (6), with  $m_q = m - 2\sigma$ . Once again the vacuum fluctuation term is regularized by means of a ultraviolet cutoff, that we denote by  $M$ . The relation between the chiral condensate and  $\sigma$  in the PNJL model is  $\sigma = 2G\langle \bar{q}q \rangle$ .

We notice that in this case we take quarks with a finite bare mass, which will be fixed by requiring that the pion mass in the vacuum is in agreement with its experimental value. We also notice that the PNJL model considered here, which is dubbed Extended-PNJL in [24], has been tuned in order to reproduce quantitatively the Lattice QCD thermodynamics at zero and imaginary quark chemical potential. Hence, it represents a faithful description of QCD, in terms of collective degrees of freedom related to chiral symmetry breaking and deconfinement.

The potential term  $\mathcal{U}$  in Eq. (14) is built by hand in order to reproduce the pure gluonic lattice data with  $N_c = 3$  [30]. We adopt the following logarithmic form,

$$\mathcal{U}[L, \bar{L}, T] = T^4 \left\{ -\frac{a(T)}{2} \bar{L}L + b(T) \ln[1 - 6\bar{L}L + 4(\bar{L}^3 + L^3) - 3(\bar{L}L)^2] \right\}, \quad (17)$$

with three model parameters (one of four is constrained by the Stefan-Boltzmann limit),

$$a(T) = a_0 + a_1 \left(\frac{T_0}{T}\right) + a_2 \left(\frac{T_0}{T}\right)^2, \quad (18)$$

$$b(T) = b_3 \left(\frac{T_0}{T}\right)^3.$$

The standard choice of the parameters reads  $a_0 = 3.51$ ,  $a_1 = -2.47$ ,  $a_2 = 15.2$  and  $b_3 = -1.75$ . The parameter  $T_0$  in Eq. (17) sets the deconfinement scale in the pure

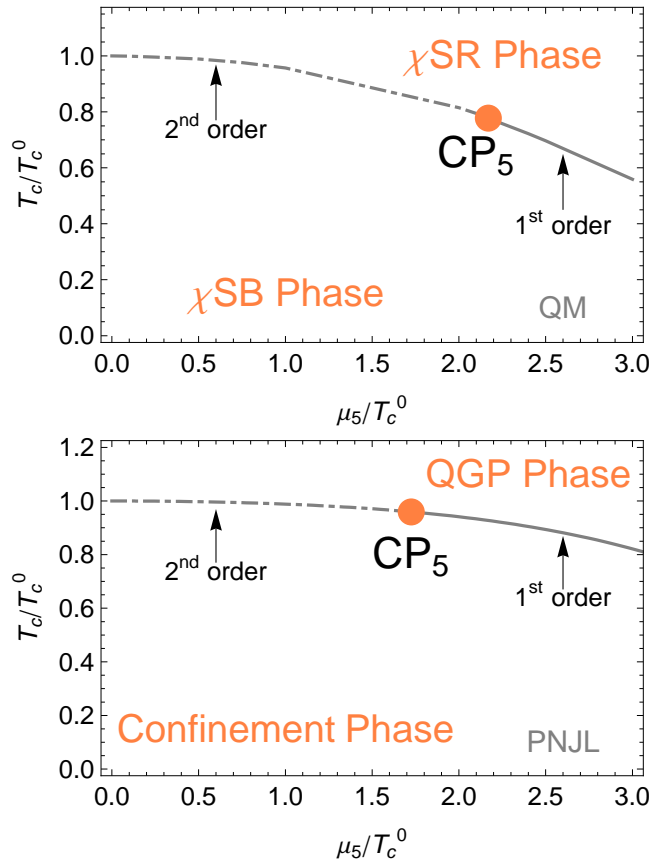


FIG. 1. (Color online). *Upper panel*: Phase diagram of the QM model in the  $\mu_5 - T$  plane. The dot-dashed line corresponds to the second order chiral phase transition; the solid line denotes the first order phase transition. The orange dot is the critical endpoint. The scale  $T_c^0 = 174.1$  MeV corresponds to the critical temperature at  $\mu_5 = 0$ . *Lower panel*: Phase diagram of the PNJL model. Lines convention is the same as in the upper panel. The scale  $T_c^0 = 173.9$  MeV corresponds to the critical temperature at  $\mu_5 = 0$ .

gauge theory. In absence of dynamical fermions one has  $T_0 = 270$  MeV. However, dynamical fermions induce a dependence of this parameter on the number of active flavors [34]. For the case of two light flavors to which we are interested here, we take  $T_0 = 190$  MeV as in [24]. Also for the remaining parameters we follow [24] and take  $M = 631.5$  MeV,  $m = 5.5$  MeV and  $G = 5.498 \times 10^{-6}$  MeV $^{-2}$ .

### III. CRITICAL ENDPOINT AT ZERO CHEMICAL POTENTIAL

In Figure 1 we plot the phase diagram of the chiral models in the  $\mu_5 - T$  plane, for the case  $\mu = 0$ . It is obtained by a minimization procedure of the full potential (5) for the QM model, and (14) for the case of the PNJL model.

In the case of the QM model, the critical temperature  $T_c$  is identified with the one at which  $\langle\sigma\rangle_{T=T_c} = 0$ . For the PNJL model, since chiral symmetry is broken explicitly by the quark mass and the phase transitions are replaced by crossovers, we identify the critical temperature with that at which  $dL/dT$  is maximum. We have checked that the latter deviates from that at which  $|d\sigma/dT|$  is maximum only of a few MeV, in the whole range of parameters studied. Even in this case, with an abuse of nomenclature, we dub the pseudo-critical lines as second order and first order, as in the case of the QM model. It is clear from the context that, whenever we talk about the PNJL model, the term second order transition has to be taken as a synonym of smooth crossover; similarly, the term first order transition is a synonym of discontinuous jump of the order parameters.

In the case of the QM model, the data about the condensates as a function of temperature at  $\mu_5 \neq 0$  have been presented already in the literature [21], therefore their reproduction in this Article would be just of academic interest; hence we skip this step here. Our focus is the discussion of the critical endpoint and of its evolution from  $\mathcal{W}_5$  to  $\mathcal{W}$ ; hence we focus on  $\text{CP}_5$  and  $\text{CP}$ .

In both panels of Figure 1, the grey dashed line corresponds to the second order chiral phase transition in the case of the QM model, or to a smooth crossover in the case of the PNJL model. The solid line, on the other hand, denotes the first order transition. The dot corresponds to  $\text{CP}_5$ . In the following, we label the coordinates of  $\text{CP}_5$  by  $(\mu_{5c}, T_{5c})$ . For the case of the QM model, since we do not have any information about confining-deconfining property of a given phase, we can label the phases of the model only in terms of the chiral symmetry. We call the phase below the critical line as the chiral symmetry broken phase; similarly, above the critical line, chiral symmetry is restored, hence we call this phase as the chiral symmetry restored phase. It is then natural that  $\text{CP}_5$  in this case is a *chiral* critical endpoint.

For the case of the PNJL model, on the other hand, we have access to the chiral condensate and to the Polyakov loop expectation value. As a consequence, we can label the phases of the model in terms both of confining properties, and of chiral symmetry. In the model at hand, because of the entanglement in Equation (13), the deconfinement and chiral symmetry restoration crossovers take place simultaneously both at value of  $\mu_5$ . This is proved by our data about  $\sigma$  and  $L$ , see Figure 2 in which we plot the chiral condensate (upper panel) and the expectation value of the Polyakov loop (lower panel) as a function of temperature, for several values of  $\mu_5$ . In [19] the two crossovers joined only for  $\mu_5 > \mu_{5c}$ . Our results are a natural consequence of the entanglement vertex in Equation (13), which was neglected in [20].

It is useful to stress that in the PNJL model we are discussing crossovers. Due to the crossover nature of the phenomena, a unique definition of the critical temperatures is not available; in this article we have used the definition which is easiest to implement, namely the

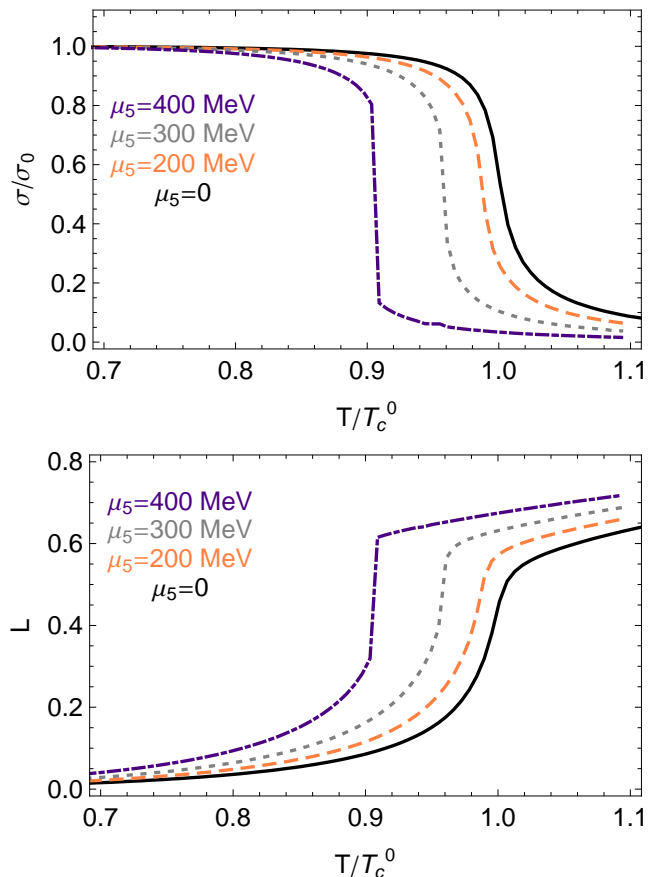


FIG. 2. (Color online). *Upper panel*: Chiral condensate in the PNJL model, normalized to the value at zero temperature, as a function of temperature for several values of  $\mu_5$ . Black solid line corresponds to the case  $\mu_5 = 0$ ; orange dashed line to  $\mu_5 = 200$  MeV; grey dotted line to  $\mu_5 = 300$  MeV; indigo dot-dashed line to  $\mu_5 = 400$  MeV. *Lower panel*: Expectation value of the Polyakov loop as a function of temperature, for several values of  $\mu_5$ . Dashing and color convention is the same as in the upper panel.

study of the peaks of the derivatives of the order parameters. We dub these quantities as effective susceptibilities. Within numerical error, we find that the peaks for the effective susceptibilities of the Polyakov loop and of the chiral condensate coincide in temperature, within few MeV. We cannot exclude that using different definitions for the pseudo-critical temperatures, like the identification of the crossovers with the peaks of true susceptibilities, the former can be shifted of some MeV, leading eventually to a larger split of the deconfinement and the crossover temperatures. However, the qualitative picture should not be modified drastically, as previous studies within the PNJL model have shown.

Because of this peculiarity of the PNJL model, at the pseudo-critical line both deconfinement and chiral restoration crossovers take place. Hence the region below the pseudo-critical line is characterized by confinement and spontaneous breaking of chiral symmetry; we label

this phase as the confinement phase. On the other hand, the phase above the critical line is identified with the Quark-Gluon-Plasma phase. In this case,  $CP_5$  is both *chiral* and *deconfinement* critical endpoint.

For what concerns the coordinates of  $CP_5$ , in the case of the QM model we find

$$\left(\frac{\mu_{5c}}{T_c^0}, \frac{T_c}{T_c^0}\right) = (2.16, 0.78), \quad CP_5 \text{ (QM)}, \quad (19)$$

where  $T_c^0 = 174.1$  MeV is the chiral symmetry restoration temperature at  $\mu = \mu_5 = 0$ . Moreover, for the PNJL model we find

$$\left(\frac{\mu_{5c}}{T_c^0}, \frac{T_c}{T_c^0}\right) = (1.73, 0.96), \quad CP_5 \text{ (PNJL)}, \quad (20)$$

where  $T_c^0 = 173.9$  MeV is the deconfinement temperature at  $\mu = \mu_5 = 0$ .

#### IV. CRITICAL ENDPOINT AT FINITE CHEMICAL POTENTIAL

Next we turn to discuss the more general case with both  $\mu_5$  and  $\mu$  different from zero. Our scope is to show that, at least within the models, CP naturally evolves into  $CP_5$ . Hence the latter, if detected on the Lattice, can be considered as the benchmark of the former. In particular the PNJL model, which is in quantitative agreement with the Lattice at zero chemical potential, gives a numerical relation among the coordinates of CP and  $CP_5$ , which might be taken as a guide to estimate the coordinates of CP in QCD, once  $CP_5$  is detected.

In Figure 3 we collect our data on the critical point of the phase diagram in the  $\mu - \mu_5 - T$  space, in the case of the PNJL model (for the QM model we obtain similar results). The orange solid line is the union of the critical points computed self-consistently at several values of  $\mu$ : at any value of  $\mu$ , a point on the line corresponds to the critical point of the phase diagram in the  $\mu_5 - T$  plane. Thus the line pictorially describes the evolution of the critical point of the chiral model at hand, from CP to  $CP_5$ . In Figure 4 we plot a projection of Fig. 3 onto the  $\mu - \mu_5$  plane, for the PNJL model. The indigo solid line corresponds to the  $\mu_5$ -coordinate of the critical endpoint. The critical temperature is not so much affected when we continue  $CP_5$  to CP (we measure a change approximately equal to the 3%), therefore the projection in the  $\mu - T$  plane is redundant.

At  $\mu_5 = 0$ , the critical point is found at the following coordinates:

$$\left(\frac{\mu_c}{T_c^0}, \frac{T_c}{T_c^0}\right) = (0.92, 0.93), \quad CP \text{ (PNJL)}, \quad (21)$$

which correspond to  $\mu_c \approx 160$  MeV and  $T_c \approx 165$  MeV, in agreement with the results of [24]. Similarly for the case of the QM model we find

$$\left(\frac{\mu_c}{T_c^0}, \frac{T_c}{T_c^0}\right) = (1.58, 0.49), \quad CP \text{ (QM)}. \quad (22)$$

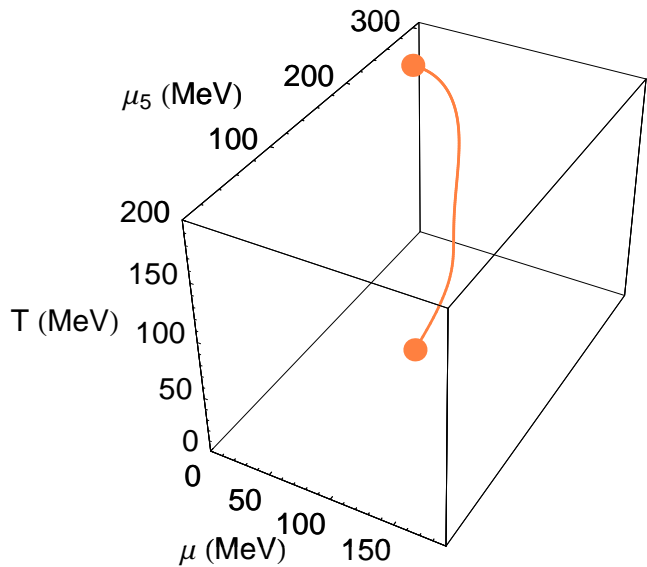


FIG. 3. (*Color online*). Evolution of the critical endpoint in the  $\mu - \mu_5 - T$  space, for the PNJL model.

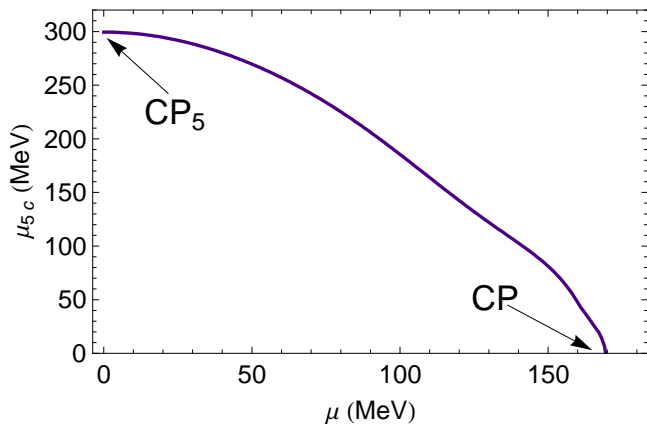


FIG. 4. (*Color online*). Projection of Fig. 3 onto the  $\mu - \mu_5$  plane, for the PNJL model. The solid line corresponds to the  $\mu_5$ -coordinate of the critical endpoint.

The natural question which arises is: suppose a grand-canonical ensemble simulation finds  $CP_5$ ; then, how can the coordinates of the latter point help to locate CP? We can answer to this important question within the PNJL model. Our numerical results, Equations (20) and (21), suggest the following relations:

$$\frac{\mu_c}{\mu_{5c}} \approx 0.53, \quad \frac{T_c}{T_{5c}} \approx 0.97, \quad \text{(PNJL)}. \quad (23)$$

Within the QM model we obtain similar relations, but

in our opinion, those in (23) are more trustable quantitatively because the PNJL model has been tuned to be in quantitative agreement with Lattice data at zero as well as imaginary chemical potential [24], a characteristic which is not satisfied by the QM model used here.

The model predictions (23) relate the coordinates of CP to those of  $CP_5$ . In particular, it is interesting that the critical temperature is almost unchanged in the continuation of CP to  $CP_5$ . Of course, since these results are deduced by a model, it is extremely interesting and important to study how Equation (23) is affected by varying parameters like the bare quark mass, or the number of active flavors. This observation opens the possibility to develop further non-academic model studies of the problem that we discuss in this Article.

## V. DISCUSSION

In this Section we summarize briefly the results obtained, and discuss their conceptual relevance, and potential applications to the Lattice as well.

Our main goal is to show that the continuation of the critical endpoint of the QCD phase diagram, CP, to a fictitious critical endpoint,  $CP_5$ , belonging to a phase diagram in the  $\mu_5 - T$  plane, is reasonable. Here  $\mu_5$  corresponds to the chiral chemical potential, which is conjugated to the chiral density imbalance,  $n_5 = n_R - n_L$ . As we have already stressed, strictly speaking  $\mu_5$  should be regarded as a pseudo-chemical potential: quark condensate in the confinement phase induces a mix among left- and right-handed quark field components. As a consequence, the conjugated quantity to  $\mu_5$ , namely the chiral charge density, is not conserved. Hence, it is legitimate to consider  $\mu_5$  as a mere mathematical artifact, and the world in which  $\mu$  is replaced by  $\mu_5$ , that we have baptized  $\mathcal{W}_5$ , as an artificial universe, not necessarily related to the physical world. This is the point of view that we adopt in this Article.

However, even accepting this minimalist point of view,  $\mathcal{W}_5$  has the quality that it can be simulated on a Lattice. Indeed, the sign problem which affects simulations of three color QCD at finite chemical potential, does not affect QCD in  $\mathcal{W}_5$  [19]. Thus, it is possible to check whether  $CP_5$  there exists or not, within first principles calculations. If Lattice simulations find  $CP_5$ , our result suggests the simplest interpretation:  $CP_5$  *would be nothing but the continuation of the critical point which there exists in QCD*. Hence we suggest to interpret  $CP_5$ , if found, as a signal of the existence of the critical point in QCD. The coordinates of CP are related to those of  $CP_5$  by Equation (23).

Furthermore, it is extremely intriguing, theoretically speaking, that the critical endpoint  $CP_5$  that we find in this study, which confirms the findings of previous studies obtained within different models, is the analytic continuation of the critical endpoint, CP, of the theory at finite quark chemical potential.

As anticipated, previous studies [20, 21] have already discussed the possible appearance of  $CP_5$ . In particular, in [20] a PNJL model in a strong magnetic background, without entanglement vertex [see Equation (13)] has been considered. In that context, the chiral chemical potential was introduced to mimic the presence of chirality imbalance induced by instantons and sphalerons transitions in the hot QCD medium. Quantitatively, our results on the critical endpoint are in agreement with those of [20].

In [21], the phase diagram in the  $\mu_5 - T$  plane has been computed within the QM model improved with the Polyakov loop. The models considered here and in [21] are different: the zero point energy is not taken into account in [21], and on the other hand we do not include the Polyakov loop in our QM model calculations. For these reasons, it is not necessary to have a quantitative agreement among our results and those of [21]. On the contrary, it is important to notice that the qualitative picture is the same, namely the existence of a critical endpoint in the  $\mu_5 - T$  plane.

In both of the aforementioned studies, the quark chemical potential  $\mu$  has not been taken into account. Therefore, the possibility to continue  $CP_5$  to CP, which is the main idea of the study illustrated in this Article, was not considered in those references.

## VI. CONCLUSIONS AND OUTLOOK

In this Article, we have suggested the possibility of continuation of the critical endpoint of the phase diagram of  $N_c = 3$  QCD, CP, to a critical endpoint dubbed  $CP_5$  belonging to a fictional world,  $\mathcal{W}_5$ , in which the quark number chemical potential is replaced by a pseudo-chemical potential,  $\mu_5$  conjugated to the chiral charge density,  $n_5$ . The universe  $\mathcal{W}_5$  has the merit that it can be simulated on the Lattice [19] for  $N_c = 3$ . This suggestion is based on concrete calculations within chiral models. In particular, we have used the PNJL model with entanglement vertex, introduced in [24], which offers a description of the QCD thermodynamics in terms of collective degrees of freedom, which is in quantitative agreement with Lattice data at zero and imaginary chemical potential.

Our main idea is that simulations in  $\mathcal{W}_5$  might reveal the existence of a critical endpoint,  $CP_5$ , in the phase diagram. Then, this critical point might be interpreted as the continuation of the critical point which is expected to belong to the phase diagram of real QCD, because of the continuity summarized in Fig. 3. Hence it would be an indirect evidence of the existence of the critical point in real QCD. Moreover, numerical predictions of the model, which connect CP to  $CP_5$ , are in Equation (23). For these reasons, the interest of the present study is very far from being only academic or purely theoretical. Our result paves the way of the mapping of the phases of Quantum Chromodynamics at finite  $\mu$ , by virtue of the phases of a fictitious theory in which  $\mu$  is replaced by  $\mu_5$ .

In our calculations there are some factors that we have

not included for simplicity, and that might be interesting to include in more complete calculations (massive quarks, vector interactions, just to cite a couple of examples). In view of a possible mapping of the phase diagram of QCD using simulations of grand-canonical ensembles in  $\mathcal{W}_5$ , it is of great interest to extend the analysis of [25, 26] about inhomogeneous condensates, to  $\text{CP}_5$ . Moreover, in our opinion it is important to understand quantitatively how the numerical predictions of the model, namely Equation (23), are affected by varying the quark masses, and

introducing a third flavor. We plan to report on these topics in the next future.

**Acknowledgements.** Part of this work was inspired by stimulating discussions with H. Warringa, who is acknowledged. Moreover, we acknowledge M. Chernodub, M. D’Elia, P. de Forcrand, R. Gatto, A. Ohnishi, A. Yamamoto and N. Yamamoto for correspondence, careful reading of the manuscript, criticism and encouragement. This work is supported by the Japan Society for the Promotion of Science under contract number P09028.

- 
- [1] M. Asakawa and K. Yazaki, Nucl. Phys. A **504** (1989) 668.
- [2] M. A. Stephanov, K. Rajagopal and E. V. Shuryak, Phys. Rev. Lett. **81** (1998) 4816; D. T. Son and M. A. Stephanov, Phys. Rev. D **70** (2004) 056001; H. Fujii, Phys. Rev. D **67** (2003) 094018; M. A. Stephanov, Phys. Rev. Lett. **102** (2009) 032301; Y. Minami and T. Kunihiro, Prog. Theor. Phys. **122** (2010) 881.
- [3] M. A. Stephanov, K. Rajagopal and E. V. Shuryak, Phys. Rev. D **60** (1999) 114028.
- [4] Z. Fodor and S. D. Katz, JHEP **0203** (2002) 014; S. Ejiri *et al.*, Prog. Theor. Phys. Suppl. **153** (2004) 118; R. V. Gavai and S. Gupta, Phys. Rev. D **71** (2005) 114014; P. de Forcrand, S. Kim and O. Philipsen, PoS **LAT2007** (2007) 178; P. de Forcrand and O. Philipsen, JHEP **0811** (2008) 012.
- [5] P. de Forcrand, PoS **LAT2009**, 010 (2009).
- [6] T. Z. Nakano, K. Miura and A. Ohnishi, Phys. Rev. D **83** (2011) 016014.
- [7] P. de Forcrand, M. Fromm, Phys. Rev. Lett. **104**, 112005 (2010). [arXiv:0907.1915 [hep-lat]].
- [8] M. A. Stephanov, PoS **LAT2006** (2006) 024.
- [9] A. Ohnishi, H. Ueda, T. Z. Nakano, M. Ruggieri, K. Sumiyoshi, [arXiv:1102.3753 [nucl-th]].
- [10] M. G. Alford, A. Kapustin, F. Wilczek, Phys. Rev. **D59**, 054502 (1999).
- [11] P. de Forcrand, O. Philipsen, Nucl. Phys. **B642**, 290-306 (2002).
- [12] M. D’Elia, M. P. Lombardo, Phys. Rev. **D67**, 014505 (2003).
- [13] P. de Forcrand, O. Philipsen, JHEP **0811**, 012 (2008); Phys. Rev. Lett. **105**, 152001 (2010).
- [14] J. B. Kogut, D. K. Sinclair, Phys. Rev. **D66**, 034505 (2002).
- [15] P. de Forcrand, M. A. Stephanov, U. Wenger, PoS **LAT2007**, 237 (2007).
- [16] P. Cea, L. Cosmai, M. D’Elia, C. Manneschi, A. Papa, Phys. Rev. **D80**, 034501 (2009).
- [17] A. Li, A. Alexandru, K. -F. Liu, [arXiv:1103.3045 [hep-ph]].
- [18] M. Hanada, N. Yamamoto, [arXiv:1103.5480 [hep-ph]].
- [19] K. Fukushima, D. E. Kharzeev and H. J. Warringa, Phys. Rev. D **78**, 074033 (2008).
- [20] K. Fukushima, M. Ruggieri and R. Gatto, Phys. Rev. D **81**, 114031 (2010).
- [21] M. N. Chernodub and A. S. Nedelin, arXiv:1102.0188 [hep-ph].
- [22] L. D. McLerran, E. Mottola, M. E. Shaposhnikov, Phys. Rev. **D43**, 2027-2035 (1991); H. B. Nielsen, M. Nomiya, Phys. Lett. **B130**, 389 (1983); A. N. Sisakian, O. Y. Shevchenko, S. B. Solganik, [hep-th/9806047]; M. Joyce, T. Prokopec, N. Turok, Phys. Rev. **D53**, 2958-2980 (1996).
- [23] K. Fukushima, Phys. Lett. **B591**, 277-284 (2004).
- [24] Y. Sakai, T. Sasaki, H. Kouno and M. Yahiro, Phys. Rev. D **82**, 076003 (2010).
- [25] D. Nickel, Phys. Rev. Lett. **103**, 072301 (2009).
- [26] A. Flachi, T. Tanaka, JHEP **1102**, 026 (2011).
- [27] J. L. Gervais and B. W. Lee, Nucl. Phys. B **12**, 627 (1969); A. L. Mota, M. C. Nemes, B. Hiller and H. Walliser, Nucl. Phys. A **652**, 73 (1999); O. Scavenius, A. Mocsy, I. N. Mishustin, D. H. Rischke, Phys. Rev. **C64**, 045202 (2001).
- [28] Y. Nambu and G. Jona-Lasinio, Phys. Rev. **122**, 345 (1961); Y. Nambu and G. Jona-Lasinio, Phys. Rev. **124**, 246 (1961).
- [29] U. Vogl and W. Weise, Prog. Part. Nucl. Phys. **27**, 195 (1991); S. P. Klevansky, Rev. Mod. Phys. **64**, 649 (1992); T. Hatsuda and T. Kunihiro, Phys. Rept. **247**, 221 (1994); M. Buballa, Phys. Rept. **407**, 205 (2005).
- [30] S. Roessner, C. Ratti and W. Weise, Phys. Rev. D **75**, 034007 (2007);
- [31] C. Sasaki, B. Friman and K. Redlich, Phys. Rev. D **75**, 074013 (2007); S. K. Ghosh, T. K. Mukherjee, M. G. Mustafa and R. Ray, Phys. Rev. D **77**, 094024 (2008); A. Bhattacharyya, P. Deb, S. K. Ghosh and R. Ray, Phys. Rev. D **82**, 014021 (2010).
- [32] H. Abuki, R. Anglani, R. Gatto, G. Nardulli and M. Ruggieri, Phys. Rev. D **78**, 034034 (2008).
- [33] K. Kashiwa, H. Kouno, M. Matsuzaki and M. Yahiro, Phys. Lett. B **662**, 26 (2008);
- [34] T. K. Herbst, J. M. Pawłowski and B. J. Schaefer, arXiv:1008.0081 [hep-ph].
- [35] T. Kahara and K. Tuominen, Phys. Rev. D **78**, 034015 (2008); Phys. Rev. D **80**, 114022 (2009); arXiv:1006.3931 [hep-ph].
- [36] V. Skokov, B. Friman, K. Redlich, [arXiv:1008.4570 [hep-ph]]; V. Skokov, B. Friman, E. Nakano, K. Redlich, B. - J. Schaefer, Phys. Rev. **D82**, 034029 (2010).
- [37] J. O. Andersen, R. Khan, L. T. Kyllingstad, [arXiv:1102.2779 [hep-ph]].
- [38] H. D. Politzer, Nucl. Phys. B **117**, 397 (1976); Phys. Lett. B **116**, 171 (1982).
- [39] K. I. Kondo, Phys. Rev. D **82**, 065024 (2010).
- [40] M. Frasca, arXiv:0803.0319 [hep-th]; arXiv:1002.4600 [hep-ph].



- [41] J. Braun, A. Janot, [arXiv:1102.4841 [hep-ph]].
- [42] M. D'Elia and F. Sanfilippo, Phys. Rev. D **80**, 111501 (2009).
- [43] C. Bonati, G. Cossu, M. D'Elia and F. Sanfilippo, arXiv:1011.4515 [hep-lat].